RSC Advances

PAPER

View Article Online
View Journal | View Issue

Cite this: *RSC Adv.*, 2021, **11**, 24206

A highly efficient chemical approach to producing green phosphorylated cellulosic macromolecules†

El-Houssaine Ablouh, *[a] François Brouillette,[b] Moha Taourirte,[c] Houssine Sehaqui,[a] Mounir El Achaby [a] and Ahmed Belfkira[c]

The introduction of phosphate groups into cellulosic fibers allows for the tuning of their fire resistance, chelating and metal-adhesion properties, enabling the development of flame-retardant adhesive and adsorbent materials. Toward that end, the major challenge is developing a novel efficient and environmentally friendly phosphorylation route that offers an alternative to existing methods, which can achieve the targeted properties. For this purpose, cellulosic fibers were chemically modified herein using solid-state phosphorylation with phosphoric acid and urea without causing substantial damage to the fibers. The morphological, physicochemical, structural and thermal characterisations were examined using FQA, SEM, EDX, FTIR, $^{13}C/^{31}P$ NMR, conductometric titration, zeta potential measurement and thermogravimetric analysis. All the characterisations converge towards a crosslinked polyanion structure, with about 20 wt% grafted phosphates, a nitrogen content of about 5 wt% and a very high charge density of 6608 mmol kg^{-1}. Phosphate groups are linked to cellulose through a P–O–C bond in the form of orthophosphate and pyrophosphates. Furthermore, thermal properties of the phosphorylated cellulosic fibers were investigated and a new degradation mechanism was proposed.

Received 7th April 2021
Accepted 29th June 2021

DOI: 10.1039/d1ra02713a

rsc.li/rsc-advances

1. Introduction

Recently, scientific research has focused significant efforts on the use of natural cellulosic fibers that can replace synthetic-based products.[1–3] The production of performant functional materials is a significant challenge due to the increasing demand for sustainable and eco-friendly products.[4–7] Within this philosophy, the most abundant biopolymer available on earth has attracted considerable attention and offers many advantages, such as its biodegradability, recyclability and renewable character.[8] Cellulose fibers are a type of a biopolymeric material that has been used by humans for a long time in a wide range of applications, such as clothing,[8] packaging,[9] textiles,[10] food,[11] drug release,[12] the energy sector[13–15] and the environment.[16–18] However, their hydrophilic nature and their high flammability can be problematic for many applications.[4] Consequently, there is a renewed and emergent interest in cellulose derivatives due to the inexhaustibility of this raw material. Among the more prominent cellulose derivatives are cellulose phosphates,[19] which can be obtained by chemical treatments that introduce phosphate groups onto cellulose fibers.[20–24] This modification is an essential step in order to obtain some needed properties, which are not normally found in the original cellulose structure. Thus, phosphorylated cellulose fibers have many advantageous properties that render them highly promising in many applications, such as composites,[25] flame retardant materials[3,5,26–28] and filters for the removal of heavy metals.[29,30]

The hydroxyl groups in the cellulosic chain can be modified and functionalised *via* diverse chemical pathways, some requiring low energy consumption that is necessary to produce greener fibers with new and required properties. Chemical phosphorylation is one of these methods,[3,5,8,24,31] which are categorised based on the location of the attack: either on the hydroxyl groups or by anhydroglucose unit (AGU) ring opening.[32] This chemical method has been well-documented in recent studies that have frequently employed phosphorylating agents, such as phosphate esters,[33] $(NH_4)_2HPO_4$,[3] H_3PO_4 (ref. 25) and P_2O_5.[34] This method can be performed under homogeneous conditions or heterogeneous conditions with or without a swelling step in order to achieve the partial or uniform functionalisation of the biopolymer chains.[35] Many routes for the phosphorylation of cellulosic materials have been developed, such as phosphorylation assisted by microwaves,[13] the mechanochemical ball-milling method[5] and heterogeneous or homogeneous media using a phosphate salt and phosphoric

[a]*Materials Science, Energy and Nanoengineering Department (MSN), Mohammed VI Polytechnic University (UM6P), Lot 660 – Hay Moulay Rachid, Benguerir, 43150, Morocco. E-mail: elhoussaine.ablouh@um6p.ma; lhoussainiblah@gmail.com*

[b]*Innovations Institute in Ecomaterials, Ecoproducts, and EcoEnergies – Biomass Based (I2E3), Université du Québec à Trois-Rivières, Box 500, Trois-Rivières, QC G9A 5H7, Canada*

[c]*Laboratory of Bioorganic and Macromolecular Chemistry, Department of Chemistry, Faculty of Sciences and Technology, Cadi Ayyad University, Marrakesh, 40000, Morocco*

† Electronic supplementary information (ESI) available. See DOI: 10.1039/d1ra02713a

acid.[22,24,31,36,37] The latter approaches are usually applied as chemical reactions using organic solvent or urea.[38,39]

In other methods, it is necessary to use non-toxic compounds to ensure that the fibers chains have the desired properties.[11] Therefore, a promising green ecological approach is the modification by the phosphoric acid–urea reaction system using water as the solvent. The reactivity of the cellulosic chains in this route is increased, while the cellulose degradation is decreased through the incorporation of urea as a catalyst and a swelling agent.[40] However, the phosphorylation efficiency is improved by incorporating phosphate groups into the cellulosic structure; this results in a high phosphorus content in terms of the highest degree of substitution, which is defined as the average number of substituted functional groups per AGU unit.[8] Moreover, the heterogenic reaction occurs solvent-free in a urea melt with phosphoric acid.[22,32] According to previous studies, the problem with this method is that there is a significant risk of degradation of the cellulosic materials; therefore, there is a low degree of substitution.[24] Only a few studies have tried to improve this route by optimising the molar ratio of the reagent (cellulosic fibers/phosphoric acid/urea), time, temperature and functionality in order to achieve a high degree of substitution without fibers degradation.[22,36] One of the solutions to this problem is to develop this approach in such a way that there is good contact between the fibers and the phosphorylating agent under the homogenisation temperature with a short reaction time.

In this respect, our study aimed to describe a simple, greener and previously unexplored route for direct phosphorylation of cellulosic fibers in order to increase the phosphorus content and avoid degradation of the structure of the fibers. Toward that end, the alternative phosphorylated samples were obtained by reacting cellulosic fibers with phosphoric acid and urea in two consecutive steps: (1) mixing the reagents with water to enhance the fibers swelling followed by water evaporation and (2) curing the dried sample under vacuum conditions at an optimised temperature to prevent the degradation phenomenon and to achieve structurally well-defined phosphorylated fibers. Detailed characterisation of the prepared phosphorylated fibers was obtained by solid-state nuclear magnetic resonance (^{31}P and ^{13}C NMR), Fourier transform infra-red attenuated total reflectance (FTIR-ATR) spectroscopy, scanning electron microscopy coupled with energy-dispersive X-ray analysis (SEM-EDX), fibers length distribution (FQA) thermogravimetric analysis (TGA) and zeta-potential measurement. Finally, we employed conductometric titration to define the total charge density.

2. Experimental section

2.1 Materials

The cellulosic materials used in this study are bleached softwood Kraft (PK) fibers supplied by Kruger Wayagamack (Trois Rivières, Canada). All chemical reagents were used as received from Sigma Aldrich suppliers: phosphoric acid (85%) and urea (ACS reagent 99%). Deionized water was used in all reactions. Hydrochloric acid and sodium hydroxide are of analytical grade, supplied by Analar Normapur.

2.2 Phosphorylation of cellulosic fibers

The cellulosic fibers (PK) are first washed with sodium hydroxide solution (0.1 M) to remove low molecular weight organic acids. In a flask containing 50 mL of deionized water, we introduced the three components: dry cellulosic fibers (PK), H_3PO_4 and urea (Table 1). To keep the molar ratio constant and to have intimate contact between the different components of the phosphorylation reaction, 1 g of PK fibers was impregnated with the reaction mixture. After 24 hours, the water is evaporated off under vacuum using a rotavapor (Heidolph Hei-VAP, Germany) at 90 °C. Once the water has been removed, the remaining solid is heated in the flask by raising the temperature of the rotavapor bath to 120 °C for 2 hours under vacuum. The phosphorylated cellulosic fibers (PKP) are dispersed and washed several times with deionized water to remove unreacted reagents.

2.3 Characterization techniques

2.3.1 Nuclear magnetic resonance (^{13}C/^{31}P NMR). Varian 300 INOVA spectrometer with Cross-Polarized Magic Angle Spinning (CPMAS) techniques for samples in the solid state was used to perform ^{13}C NMR measurements. Spectra were recorded at a frequency of 100 MHz. The solid-state ^{31}P (CPMAS) NMR were recorded on a Bruker DPX spectrometer at a frequency of 161 MHz. The chemical shift values were referenced to H_3PO_4 which is allocated to the 0 ppm value. All spectra were attained at a spin rate of 10 kHz.

2.3.2 Scanning electron microscopy with energy-dispersive X-ray analysis (SEM-EDX). Surface morphology of cellulosic fibers before and after phosphorylation process was done with TESCAN-VEGA3 scanning electron microscopy at an accelerating voltage of 20 kV. Energy dispersive X-ray (EDAX) analyzer was employed to depict the specific elemental composition and distribution in phosphorylated cellulosic fibers. Using an accelerating voltage of 20 kV with SEM magnification (5000×). The elemental mapping of representative areas was performed at 135 eV resolution and 0.96 μs amplification time. All samples were attached on SEM specimen holders with double-sided carbon tape and coated with gold by using high vacuum sputter coater.

2.3.3 Thermogravimetric analysis (TGA). The thermal properties of phosphorylated fibers (PKP) were also studied by using thermogravimetry (TA-TGA55). The thermal stabilities of the sample (10 mg) were evaluated under nitrogen flow (60 mL min^{-1}), from 30 to 600 °C with a heating rate of 10 °C min^{-1}.

Table 1 Molar ratios used for the phosphorylation reaction of PK fibers at 120 °C for a period of 2 h

Samples	PKP1	PKP2	PKP3	PKP4	PKP5
Molar ratio (PK : H_3PO_4 : urea)	1 : 2 : 4	1 : 2 : 10	1 : 2 : 16	1 : 3 : 4	1 : 2 : 0

Approximately 10 mg was placed in open platinum pans. It should be pointed out that all samples were thoroughly dried under identical conditions prior TGA test.

2.3.4 Attenuated total reflection Fourier transform infrared spectroscopy (ATR-FTIR). The functional groups of fibers were analyzed using Fourier Transform Infrared Spectroscopy (FTIR, Jasco-6030) operated at 2 cm^{-1} over a range of 4000–400 cm^{-1} by attenuated total reflection (ATR).

2.3.5 Total charge determination. A conductometric titration was used to determine the total charge density of the phosphorylated fibers. Before carrying out the assay, the fibers were dispersed in their acid form in a 1 mM sodium chloride solution. The assay was carried out with a sodium hydroxide solution (0.1 M) using a Thermo (USA) Orion conductometer (model 150) and a Metrohm Brinkmann (USA) automated titrator (Dosimat 765) under an inert nitrogen atmosphere.

2.3.6 Zeta-potential measurement. The measurements of the zeta potential as a function of the pH were carried out using a Malvern Zetasizer Nano ZS instrument. For this measurement, a capillary cell of zeta cells (product no. DTS1070, Malvern Instruments) was used. The phosphorylated fibers suspensions were diluted to 0.05 wt% and sonicated for 10 min before being analyzed. Then, NaCl was added to each sample until the final concentration reached 1 mM. After decanting for 20 min, the pH value of the paste was recorded and the supernatant was collected for zeta potential measurements.

2.3.7 Fiber length distribution. The variations in the dimensions of the cellulosic fibers before and after phosphorylation were determined by fiber quality analysis (FQA) of Lorentzen & Wettre Fiber Tester Plus. The average dimensions of the fibers were reported: arithmetic length, diameter, percentage of fines.

3. Results and discussion

3.1 Morphological and length distribution of phosphorylated cellulosic fibers

The surface state of unmodified and modified fibers was studied by means of SEM. The images obtained gave us an idea on the degree of modification undergone by the fibers. For the native fibers (Fig. 1a), we have images similar to those observed by other authors in previous studies.[22,36,41] A smooth surface can be seen without damaged areas. On the other hand, the SEM micrographs of the phosphorylated cellulosic fibers, for different molar ratios (1/2/4, 1/2/10 and 1/3/4), show surfaces with modifications related to the molar ratio of the different components of the phosphorylation reaction. During the reaction, the cellulose chains constituting the fibers, especially the amorphous regions, in addition to the grafting of phosphate groups, undergo degradation reactions, essentially chain cuts. These two combined actions, in addition to the phenomenon of osmosis, contributes to the erosion, thinning or even degradation of fibers. At high magnification, it is possible to observe the degree of modification undergone by the fibers according to the urea and phosphoric acid level. The surfaces of fibers obtained using the molar ratios 1/2/4 and 1/2/10, represented in Fig. 1b and c, respectively, suffered little damage compared to the fibers obtained with a molar ratio of 1/3/4. The image

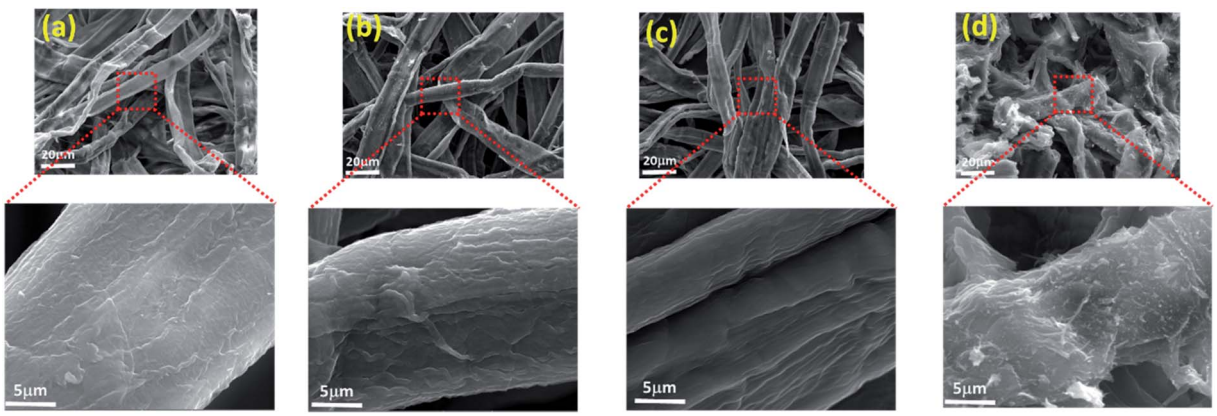

Fig. 1 Scanning electron microscopy micrographs at different magnifications of the surface view of (a) PK, (b) PKP1, (c) PKP2 and (d) PKP4.

Table 2 Measured properties of phosphorylated cellulosic fibers

Samples	Average length (mm)	Average diameter (µm)	Arithmetic length (mm)	Average fine fibers (%)	Arithmetic fine (%)
PK	1.523 ± 0.026	28.6 ± 1.072	0.824	47.5	97.4
PKP1	0.666 ± 0.011	32.0 ± 2.103	0.481	62.0	97.5
PKP2	0.856 ± 0.023	29.5 ± 1.922	0.594	42.9	96.3
PKP3	0.655 ± 0.016	28.1 ± 1.180	0.476	60.3	97.5
PKP4	0.510 ± 0.009	35.1 ± 2.263	0.381	86.7	99.3

corresponding to this latter ratio (Fig. 1d), shows an accentuated degradation of the fibers. We can say, by referring to the surface state of the fibers, that the ideal phosphorylation ratio is 1/2/10. This is confirmed by the other analyses. The length of the fibers is not affected enough, and the fixed phosphate level is optimum for this ratio (around 20%).

The length and distribution of the cellulosic fibers of the various samples were determined using a Fiber Quality Analyser (FQA). Table 2 gives the average fiber length and the percentage of fines, measured before and after phosphorylation. These measurements make it possible to evaluate the effect of the cleavage of the fibers with the chemical reactions carried out on the fiber. The increase in fine percentage is due to erosion of the fiber surfaces, as we have discussed before. In addition to degradation during phosphorylation reaction, the grafting of phosphates at the fiber surfaces makes them hydrophilic, which causes a strong absorption of water with the phenomenon of osmosis. The combined action of the various mechanical operations during the reaction (stirring, filtration, washing, *etc.*) causes the phenomena of the erosion of the surfaces of the fibers and, consequently, an increase in fines. The results grouped in Table 2 are in agreement with the images obtained with SEM. Fibers treated with a 1/2/10 molar ratio (PKP2) have a greater average length than those of other phosphorylated fibers. The increased amount of acid (PKP4) does more damage by causing the severe degradation of the fibers. Also, the diameter of the treated fibers, compared to that of the untreated fibers, is slightly larger. This is likely due to swelling caused by osmosis.

3.2 Elemental analysis and mapping of modified cellulosic fibers

Energy dispersive X-ray, ICP-OES and Kjeldahl method analyses were performed to determine chemical composition of phosphorylated fibers. The comparison of the percentages of the various elements likely to be present at the surface, before and after the phosphorylation reaction, allows us to determine the degree of the grafting of the phosphate and nitrogen groups. The EDX spectrum of unmodified fibers (PK), taken as a reference, shows only two peaks corresponding to the elements C and O (Fig. S1†). In addition, the phosphorylated samples show other peaks corresponding to phosphorus and nitrogen. The intensities of the different peaks are proportional to their

Table 3 Data of nitrogen and phosphorus contents DS_P, DS_N values

	Nitrogen content (%)				Phosphorus content (%)			
	EDX		Kjeldahl method		EDX		ICP	
Samples	N	$DS_{N(EDX)}$	N	$DS_{N(KJ)}$	P	$DS_{P(EDX)}$	P	$DS_{P(ICP)}$
PK	—	—	—	—	—	—	—	—
PKP1	4.09 ± 2.06	0.54	5.21 ± 0.01	0.71	14.87 ± 3.70	1.26	16.17 ± 3.30	1.44
PKP2	4.94 ± 2.75	0.67	5.41 ± 0.27	0.75	19.23 ± 4.77	1.99	22.08 ± 0.61	2.68
PKP3	6.85 ± 2.94	1.00	7.81 ± 0.37	1.19	18.92 ± 5.20	1.93	21.59 ± 1.06	2.54
PKP4	4.37 ± 3.06	0.58	5.67 ± 0.06	0.79	11.05 ± 5.11	0.80	12.02 ± 1.41	0.90
PKP5	0.00	0.00	0.56 ± 0.12	0.06	0.00	0.00	2.01 ± 0.49	0.11

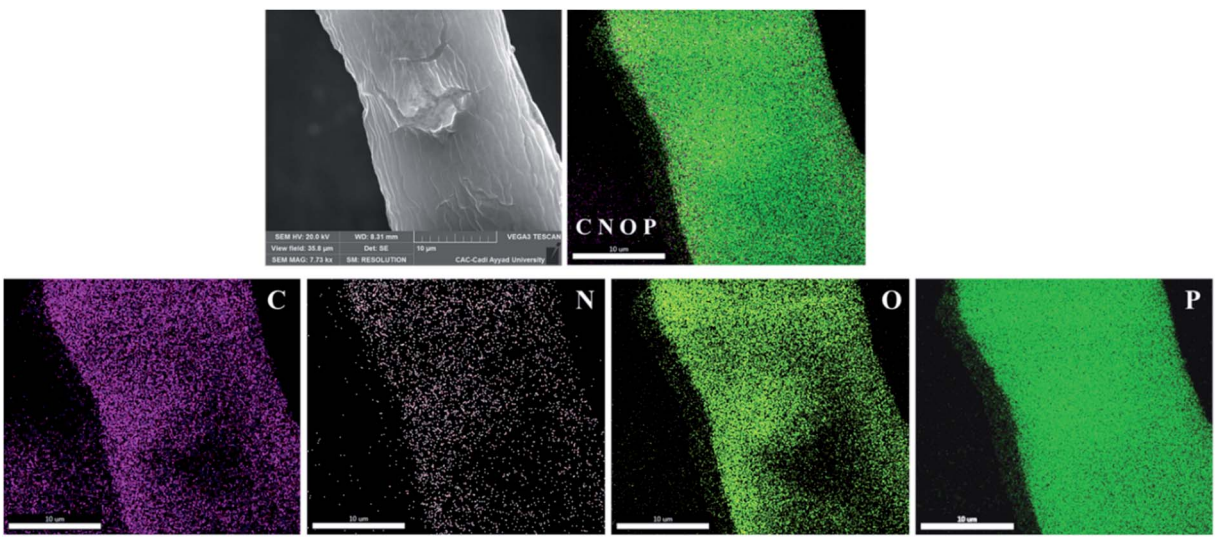

Fig. 2 Elemental mapping for carbon, oxygen, nitrogen, and phosphorus in phosphorylated cellulosic fibers PKP2.

presence on the surface. There is a decrease in the percentages of carbon and oxygen to the detriment of a proportional increase in phosphorus and nitrogen. The levels of these two elements depend on the molar ratio of cellulosic unit, phosphoric acid and urea. The results of the analyses performed using three techniques of the various prepared samples are grouped in Table 3. It is clear that the presence of urea is necessary to carry out phosphorylation (1 : 2 : 0). The other samples show a phosphate content greater than 10%. The most interesting result is that obtained for PKP2. In fact, in addition to the high phosphate content, the length of the phosphorylated fibers is the greatest and the level of fines is lower (Table 2). The quantification of the amount of grafted phosphorus as a function of the amount of urea used clearly shows that a large proportion of the cellulosic fibers have been phosphorylated with a high percentage compared to the previous works, which do not exceed 13% of P.[20–22,36,42–47]

Moreover, we carried out several tests by varying the concentration of phosphoric acid, considering the degradation effects of cellulosic chains, which can be generated by the release of acid at high temperatures.[3] It was found that the content of the P element in the phosphorylated samples (PKP1 and PKP4) decreased sharply from 14.87 to 11.05% in an acid concentration of 2 and 3 M, respectively. A further increase in the concentration of acid affected the phosphorus content and caused severe degradation of the fibers. Therefore, the presence of urea is essential to introduce phosphate moiety to the cellulosic chains without damaging the fibers, which is confirmed by the elemental analyses performed for sample PKP5 (Table 3) where the molar ratio used is 1 : 2 : 0.

Fig. 2 represents the elementary mapping of the various atoms present at the surface of the phosphorylated fibers (PKP2). It can be seen that the phosphorus density is high and uniformly distributed. It completely covers the fibers. Likewise, nitrogen also uniformly covers the surface of the fibers with a lower density. This result is in agreement with the percentages of the various chemical elements that are present. The proposed phosphorylation method is an efficient way to homogeneously incorporate the phosphate groups on the surfaces of the PK without significant damage.

The degrees of substitution, DS_P and DS_N, per unit of glucose, were calculated with the two equations, respectively ((1) and (2)), using the phosphorus and nitrogen contents measured with elemental analysis (EDX).[10,21] The two degrees, DS_P and DS_N, of substitution are reported in Table 3. A maximum substitution is obtained for the 1/2/10 reaction mixture. This result constitutes the best compromise between a high phosphorus content and an minimum cleavage of the fibers. It is also in agreement with the mapping images since phosphorus density at the surface level is extremely high. For nitrogen, the highest value of DS_N (1.19) is obtained with the conditions of the phosphorylation of PKP3. It is probably related to the amount of urea used.

$$DS_P = \frac{162 \times P\%}{3100 - 80 \times P\%} \quad (1)$$

$$DS_N = \frac{162 \times N\%}{1400 - 43 \times N\%} \quad (2)$$

3.3 Chemical structure of phosphorylated cellulosic fibers

FTIR and NMR spectroscopy analyses, zeta-potential measurements and conductometric titration of native and various phosphorylated cellulosic fibers were performed in order to

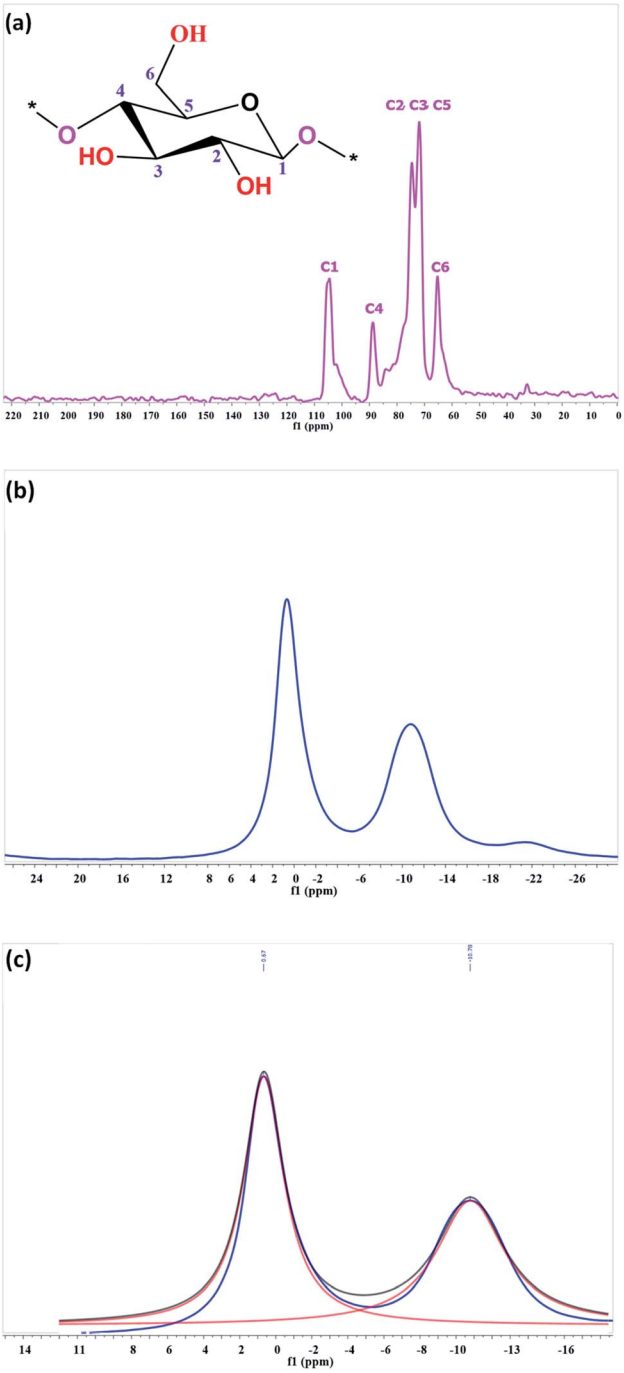

Fig. 3 Solid state ^{13}C NMR spectra (a), ^{31}P NMR spectra of phosphorylated cellulosic fiber (b) and deconvolution of sub-spectra showing peaks assigned to the orthophosphate and pyrophosphates groups (c).

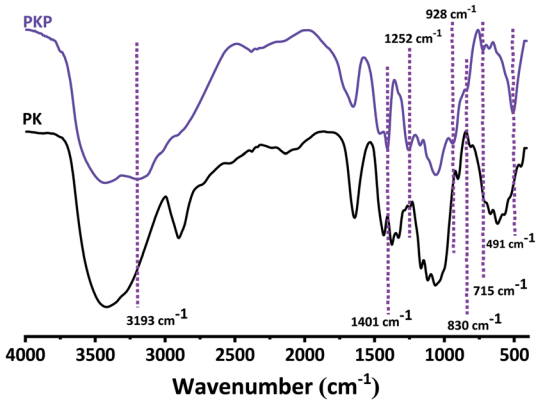

Fig. 4 FT-IR spectra of native cellulosic fibers (PK) and phosphorylated cellulosic fibers (PKP).

confirm the phosphorylation reaction. To provide more information on the structure of the phosphorylated compounds, the ^{13}C NMR analysis was carried out. Chemical shifts are sensitive to changes in the environments of each carbon. The ^{13}C NMR spectrum informs us of the modifications undergone by the carbons and the changes in their environments. The ^{13}C NMR spectrum of phosphorylated fibers shows no difference in chemical shift from that of unmodified fibers. As can be seen from the spectrum (Fig. 3a), signal and broad peak perceptible between 57 and 68 ppm correspond to the C6 of the primary alcohol group in the cellulosic cycle. The bulk chemical shift between 69 and 82 ppm is attributed to C5, C3 and C2, and the peak between 102 and 108 ppm is attributed to C1. These results are consistent with the data reported in the literature and indicate that the grafted phosphate groups do not generate specific changes in the chemical shifts of ^{13}C.[3,24,36,48]

The grafting of the phosphate groups on the cellulosic fibers is indicated by the presence of peaks in the ^{31}P NMR spectrum. According to the ^{31}P NMR data published on phosphorylated cellulosic materials, phosphorus groups appear in the region of 0–10 and −5 to 10 ppm for orthophosphate and pyrophosphates, respectively.[5,22,49,50] In our case, the spectrum of phosphorylated PKP2, using 10 moles of urea, showed clear peaks. An intense signal at 0.67 ppm is attributed to the orthophosphate groups and a less intense signal at −10.76 ppm is due to the presence of pyrophosphate groups (Fig. 3b). However, peak identification in solid-state spectra was developed with their deconvolution, resulting in one peak for orthophosphate diesters and one for pyrophosphate (Fig. 3c). The absence of a phosphoric acid peak confirmed the efficiency of the washing process with deionised water after the reaction to remove any unbound phosphate groups.

The results of the ^{31}P and ^{13}C NMR analyses were confirmed by FTIR spectroscopy (Fig. 4). The spectra all show glucosidic units. The characteristic bands at 3427, 2898 and 1051 cm^{-1} correspond to the stretching vibrations of O–H, C–H and C–O–C of the glucosidic units, respectively.[21,36,51] Another absorption around 1649 cm^{-1} is attributed to the O–H bending of the adsorbed water.[51] The sharp peak at 1428 cm^{-1} can be attributed to the C–H bending vibrations. The 667 cm^{-1} band is characteristic of the OH vibration band.[52]

The grafting of phosphate groups is accompanied by the appearance of new bands in the FTIR spectrum of phosphorylated fibers. As we have already seen with EDX, in addition to carbon and oxygen, phosphorylated fibers contain phosphorus and nitrogen. These two elements are present in the form of P═O, O–P–OH, P–O–C, P–OH, –P–NH_2, –P–NH–. The most intense of these bands is at 1401 and 1252 cm^{-1}, assigned to the vibration of P═O of the orthophosphate diester[19,38,44,53] and P═O stretching vibrations,[36,49,51] respectively. The formation of –P–NH_2 structures was confirmed by the appearance of two bands at 715 and 3193 cm^{-1}, assigned respectively to P–NH groups and stretching vibrations of N–H.[53] In addition, with regard to the phosphorylated fibers (PKP), the IR spectra exhibit new bands at 497 cm^{-1}, corresponding to the bending vibration of O–P–OH.[45] The FTIR spectrum of PKP, which also presents a characteristic absorption of 830 and 928 cm^{-1}, is indicative of the stretching mode of the P–O–C aliphatic bond[5,22] and P–OH.[42,43,51]

In addition to the sulphonate, the grafting of the phosphate groups confers the fibers a polyanionic character. It is possible

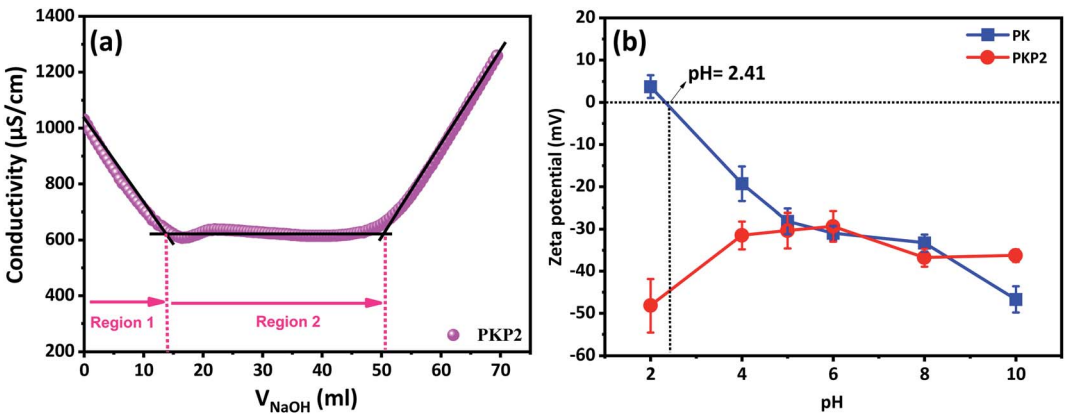

Fig. 5 Conductivity titration curve of phosphorylated lignocellulosic fibers (a) and zeta potential measurements as a function of pH for cellulosic fibers (PK) and phosphorylated cellulosic fibers (PKP2) (b).

to measure the rate of charge carried by these fibers with conductimetric titration. After being washed with deionised water several times, the phosphorylated cellulosic samples are titrated with a 0.1 N sodium hydroxide solution. The groups present at the surface of phosphorylated fibers are of three types. In addition to the acidic functions of the phosphate groups grafted onto the surface of the fibers, there are also the sulphonates and carboxylates originating from oxidation, essentially of the primary alcohol of the fibers, from chemical treatment during their production. The neutralisation of these acid functions allow us to determine the total charge content of the phosphate groups, which can provide information on the structure of phosphorylated fibers.[3,22] The change in potential as a function of the volume of the sodium hydroxide solution is shown in Fig. 5a.

The dosage of acid groups in unmodified fibers is approximately 100 μeq. g^{-1}.[33] The dosed acid functions are those of the sulfonate and carboxylate functions originating from the oxidative treatment of the fibers during the isolation and bleaching of the cellulosic fibers. Therefore, they are the first to be neutralised in an assay. The first segment (zone 1) is attributable to the neutralisation of these acid functions. The second segment, in the form of a straight line, is attributable to the neutralisation of the protons of the phosphate groups. The volume consumed during the neutralisation of these groups allows us to calculate the number of equivalents or, in other words, the charge rate. The found load rate is 6608 mmol kg^{-1}, *i.e.* 66 times more than with unmodified fibers. A large increase was generally observed in total charge content upon phosphorylation, which reached an optimal value using a molar ratio of 1/2/10 at 120 °C for two hours. To the best of our knowledge, this is among the highest charge content reported in literature for phosphorylated cellulosic fibers (Table 4).

Table 4 Total charge contents values of phosphorylated cellulosic materials

Cellulosic materials	Phosphorylating agent	Total charge contents (mmol kg^{-1})	References
Cellulose nanocrystals	P_2O_5	3300	5
Cellulose fiber	$(NH_4)_2HPO_4$	1180	24
Cellulose nanofibrils	$(NH_4)_2HPO_4$	2000	28
Nanocellulose	H_3PO_4	1173	48
Cellulose fiber	H_3PO_4	500	47
Cellulose nanofibrils	NaH_2PO_4	900	54
Cellulose nanofiber	$NH_4H_2PO_4$	1230	55
Cellulosic fibers	H_3PO_4	6608	This study

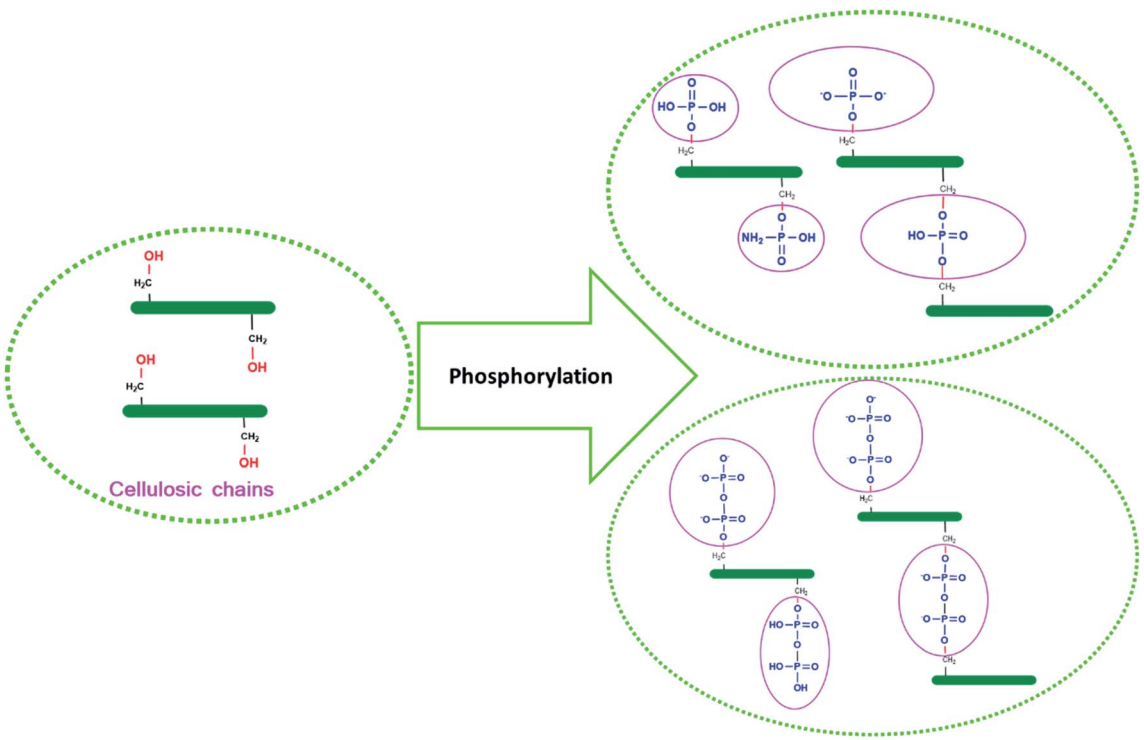

Fig. 6 Reactive scheme of phosphorylated fibers and the possible products obtained.

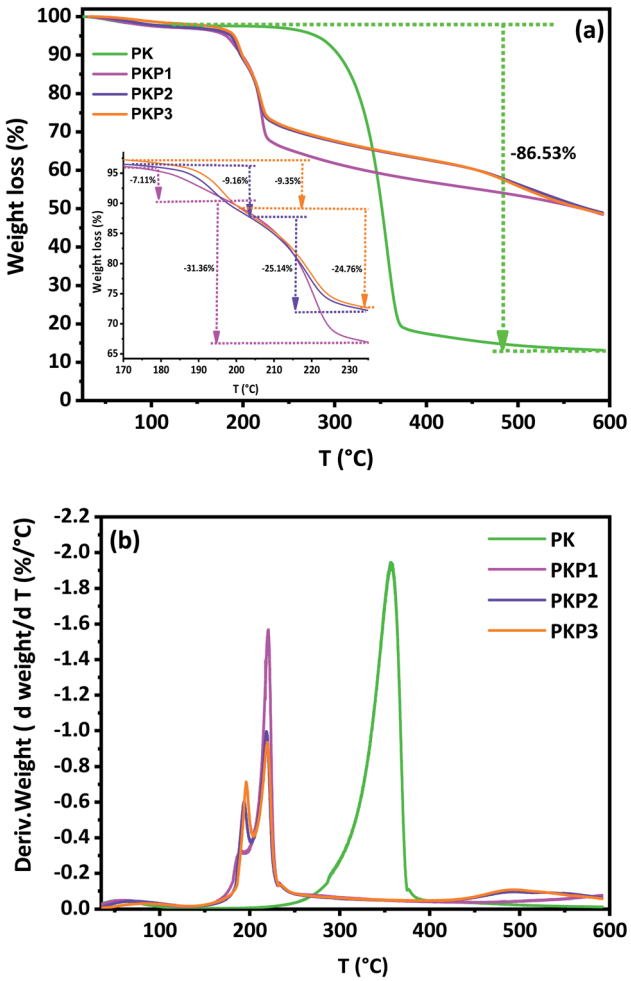

Fig. 7 TG (a) and DTG (b) curves of untreated (PK) and treated cellulosic fibers (PKP1, PKP2, PKP3).

To understand the surface charge characteristics of fibers before and after the phosphorylation process, an evolution of zeta potential, as a function of pH, was determined (Fig. 5b). The obtained results indicate that PK have positive zeta potential values with acidic pH (pH < 2.41) but are negatively charged with basic pH. This result is similar to that of previous studies, which reveal that negative charge must originate from deprotonation.[56] On the other hand, the negative charge present in PKP2 was found to be higher in absolute value than that of PK due to the increase in the contents of the introduced phosphoric groups. Most importantly, surface charge characterisation by zeta potential not only further confirms the successful phosphorylation of PK but is also more sensitive to show surface changes from the introduced phosphates groups. The potential applications of this type of materials are numerous, for instance, cation exchange medium with its high charge and large hydrodynamic volume in aqueous media. Moreover, such materials can be used in different formulations: in water-based paints as a dispersing agent, stabiliser and rheological agent. The problems with the stability of emulsions and products can be solved with this type of product. The results of structural characterisation and the physico-chemical analysis of the PKP led us to propose an approximate structure after phosphorylation (Fig. 6).

3.4 Thermal studies of phosphorylated fibers

Phosphorylated fibers are products that have anti-fire properties. Several studies have shown that the presence of phosphate groups prevent the spread of flames by preventing the diffusion of the oxidant, oxygen, inside the material.[25,27,40,57] The phosphate groups form a protective shell. To better understand the mechanism of decomposition and the formation of the protective layer by the phosphate groups, we refer to what has already been done in this field.

The monitoring of the decomposition of cellulose as a function of temperature and the analysis of the products formed during decomposition have shown that, primarily, dehydration, rearrangements and depolymerisation occur. At temperatures below 400 °C, the monomeric repeating unit cellobiose mainly transforms into levoglucosan.[33,45] The examination of Fig. 7 and S2† shows that the introduction of phosphate groups lowers the onset of decomposition towards low temperatures. We have recorded the various successive losses in Table 5 and the temperature intervals at which they occur.

While unmodified cellulosic fibers are characterised by two maximum mass-loss temperatures, phosphorylated cellulosic fibers displayed four degradation stages (Fig. 7b). The two temperatures (T_{max}/°C) of PK are 54 °C and 357 °C, which correspond successively to the mass losses (Δm/%) of water adsorbed by the fibers (1.87%) and the decomposition of cellulose chains (84.66%). In addition to the loss of water, the

Table 5 Thermal parameters of the obtained phosphorylated cellulosic fibers from TGA analysis in N_2 atmosphere

	First stage		Second stage		Third stage		Fourth stage		
Samples	T_{max} (°C)	Δm (%)	T_{max} (°C)	Δm (%)	T_{max} (°C)	Δm (%)	T_{max} (°C)	Δm (%)	Residue at 600 °C (%)
PK	54	1.87	357	84.66	—	—	—	—	13.46
PKP1	60	2.86	189	7.11	221	31.36	—	10.30	48.37
PKP2	71	2.73	193	9.16	218	25.14	490	13.08	49.89
PKP3	82	2.62	196	9.35	220	24.76	492	15.02	48.25
PKP4	74	2.13	193	5.44	225	29.01	—	16.54	46.88
PKP5	62	1.97	340	86.91	—	—	—	—	11.12

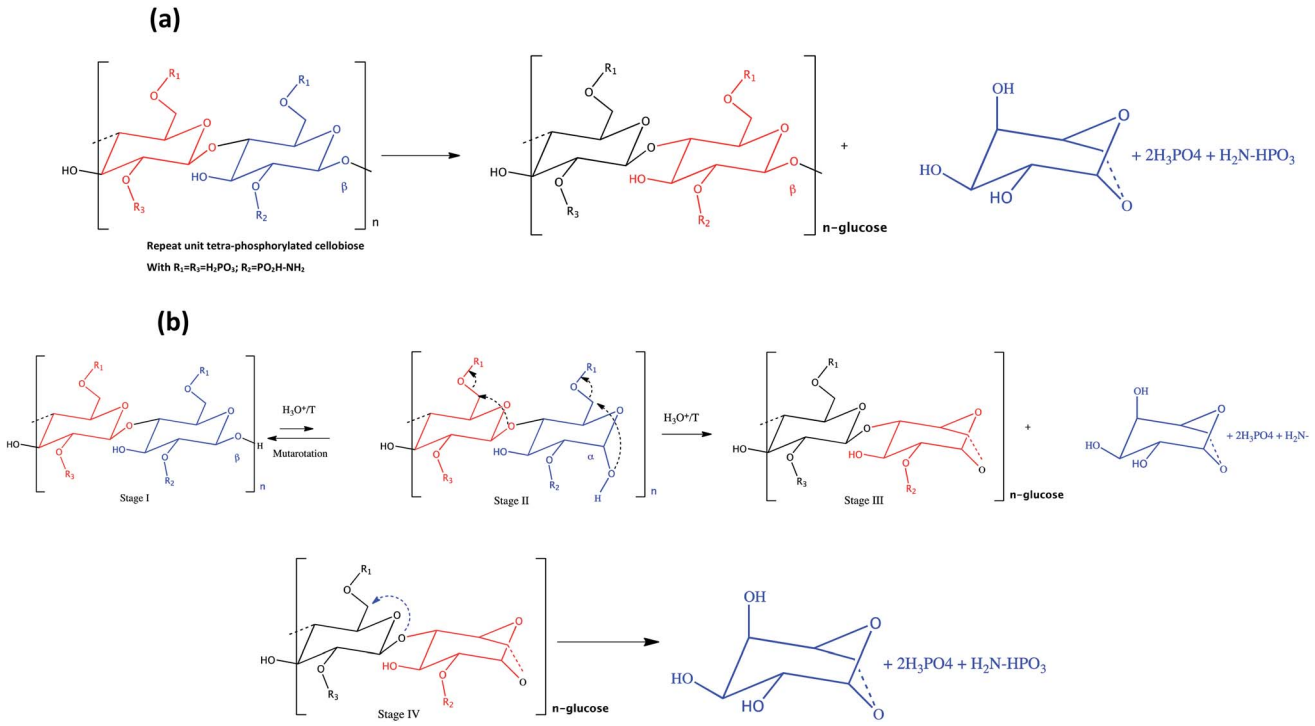

Fig. 8 (a) Repeating unit and formation of levoglucosan, and (b) mechanism of depolymerization of phosphorylated cellulosic chains.

phosphorylated fibers exhibit three degradation stages characterised by different temperatures (T_{max}/°C) and losses (Δm/%), as can be seen in Table 5 and Fig. S3.† The total loss represents about 50% at 600 °C. This behaviour of PKP is well known; thermal degradation and early charcoal formation are responsible for the resistance to fire propagation of materials containing phosphates.

In a previous work, we focused on the empirical mechanism proposed by various researchers to explain the degradation of phosphorylated fibers and the formation of the protective layer.[33] It appears from these studies that there is first a release of phosphoric acid into the medium. With the combined effect of phosphoric acid and temperature, classic dehydration reactions take place. There is formation of unsaturation in the repeating units of the cellulose chains. The presence of hydroxyls of the glucopyranose and of the newly created unsaturation promote the formation of carbonyl groups through a keto–enol balance.[58]

Also, a highly phosphorylated sample with a phosphorus content of about 20% ($DS_P > 2$) begins to decompose at lower temperatures than unmodified cellulosic fibers. The first step with a mass loss (Δm/%) of 2.73 at a temperature T_{max} of 71 °C corresponds to the loss of water that has been adsorbed. The quantity of water and the temperature associated with this phenomenon are higher than those of PK alone. This is a predictable result, given the presence of highly polar and hydrophilic phosphate groups. The second mass loss of 9.16%, at a temperature of 193 °C, corresponds to dehydration reactions accompanying the departure of phosphoric acid (Fig. 7b). Indeed, it has been shown that the first group that leaves the phosphorylated chains is the phosphate group;[33] of the four phosphate groups grafted onto the repeating unit of the cellulose chains of the fibers, we believe that those located in the C2 carbon, the most crowded region, without free rotation, are the first to leave. Studies carried out on polystyrene show that the grafting of acetate groups in the alpha carbon of styrene (α-acetoxystyrene) causes the polystyrene chain to lose all flexibility. Poly α-acetoxystyrene has no glass transition or melting temperature, and releases acetic acid at 170 °C.[59] This is mainly due to the steric hindrance created by the acetoxy group on the polystyrene chain. Phosphate groups of C6, where there is less steric hindrance, require more energy and are released secondly under the combined acid and temperature effect. The conditions are favourable (high temperature, acidic medium and presence of hydroxyls) for reactions, especially dehydration, levoglucosan formation, depolymerisation and others, such as rearrangements.

A study was carried out in 2009 to determine the nature of the products formed during the heat treatment of cellulose.[60] The number of products detected with the gas-chromatography technique exceeded 100. But the majority of products are in the following order: levoglucosan (53%), hydroxyacetaldehyde (8.7%), hydroxyacetone (3.4%) and acetone (3%). The formation of levoglucosan is thermodynamically favoured by the chain-end mechanism due to the lowest energy barrier.[61] The second weight loss (9.16%) is attributed to the dehydration of anhydroglucose and, at the same time, to depolymerisation and the formation of levoglucosan. Also, the phosphoric acid formed undergoes a condensation reaction at this temperature.[62] The third loss of 25.14% is attributed to the formation

and evaporation of levoglucosan. Indeed, its molar mass is 162 g mol^{-1} and the mass of the starting repeating unit, tetraphosphorylated cellobiose, is 662 g mol^{-1}. The percentage that represents the loss of levoglucosan is $(162/662) \times 100 = 24.47\%$. This result fits well with our previous study.[33]

With the significant conversion of organic mass, almost 50%, we assume that there is a regular mechanism, not random like the radical mechanism, of formation of a product (levoglucosan in this case). It is a chain reaction of depolymerisation promoted by the presence of the C6 phosphate group. This phosphate group is a good nucleofuge and facilitates attacks of the oxygen doublet of the α-hydroxyl of C1, at the end of the cellulose chain, on the highly electrophilic C6 carbon. This mechanism can take place more easily if the hydroxyl group of C1, at the end of the cellulose chain, is in position α. Due to mutarotation equilibrium, more than 36% of the hydroxyl of C1 is in position α and 70% in position β. Indeed, in position α, it is much closer to C6 and can make a nucleophilic attack, facilitated by electrophilic and accentuated by the electronegative phosphate group. In position β, the hydroxyl of C1 is more distant and it is difficult to imagine such an attack. We believe that under the conditions of the reaction, there is enough energy for this reaction to take place. We propose a mechanism for the formation of levoglucosan, the main product, in 3 stages (Fig. 8). The first stage is the modification of the position of the hydroxyl of C1, from position β to α. The second step is the attack of the oxygen doublet of the hydroxyl of C1 on C6 and departure of the phosphate. The last step is the hydrolysis of the anhydroglucose and levoglucosan bond. It is a chain depolymerisation mechanism.

The rest of the product is composed of non-volatile products such as phosphates and cellulosic fibers modified into heavy compounds, mainly charcoal. Their heat treatment at 490 to 600 °C generates a remaining 49% residue. The mass loss between 490 and 600 °C is 13.08%. We believe that during this heat treatment, the most probable reaction is the polycondensation of the phosphate groups into polyphosphate P_4O_{10}, with the elimination of water and CO from organic residues and others.

4. Conclusion

The application of phosphorylated cellulosic materials has already shown great promise in the field of materials science and constitutes a greener alternative for the environment. In this study, we expanded this repertoire with the elaboration of novel eco-friendly phosphorylated cellulosic fibers, which have been successfully fabricated by an improved solid-phase modification method – a simple approach and an environmentally friendly route with great efficiency compared to those cited in literature. For the first time, the final phosphorus and nitrogen contents of prepared phosphorylated fibers can reach approximately 20 and 5%, respectively, with a maximum DS_P value of 2.68. Also, there was a high value of total charge content upon phosphorylation, which reached an value of 6608 mmol kg^{-1}. The negatively charged PKP was confirmed with zeta-potential measurement, which makes it a promising ion-exchange material. SEM results clearly show that phosphorylation reaction prevents the cleavage of the fibers and preserves its initial surface morphology. By using the results obtained from the detailed application of the $^{13}C/^{31}P$ NMR spectra, in combination with the results from FTIR studies, it has been demonstrated that the reaction between cellulosic fibers and phosphoric acid results in surface orthophosphate and pyrophosphates groups, either with crosslinking or grafting.

It was also shown that the thermal properties of phosphorylated cellulosic fibers are largely different compared to those of PK, as they form more residues and they significantly suppress the release of low-molecular toxic combustible gases. The greatest benefit of this new approach is the obtained non-degraded fibers with high phosphorus and nitrogen contents, whose properties fit the phosphorylated PK-targeted application, especially in flame-retardancy and ion-exchange materials.

Conflicts of interest

There are no conflicts to declare.

Acknowledgements

We would like to thank Dr Ahmed Radi, Cadi Ayyad University, for reviewing the linguistic aspects of this article.

References

1 J. R. G. Navarro, J. Rostami, A. Ahlinder, J. B. Mietner, D. Bernin, B. Saake and U. Edlund, *Biomacromolecules*, 2020, **21**, 1952–1961.
2 M. Ghanadpour, F. Carosio, M. C. Ruda and L. Wågberg, *ACS Appl. Mater. Interfaces*, 2018, **10**, 32543–32555.
3 M. Ghanadpour, F. Carosio, P. T. Larsson and L. Wågberg, *Biomacromolecules*, 2015, **16**, 3399–3410.
4 T. P. Molaba, S. Chapple and M. J. John, *J. Appl. Polym. Sci.*, 2016, **133**, 1–10.
5 B. G. Fiss, L. Hatherly, R. S. Stein, T. Friščić and A. Moores, *ACS Sustainable Chem. Eng.*, 2019, **7**, 7951–7959.
6 E. Ablouh, Z. Hanani, N. Eladlani, M. Rhazi and M. Taourirte, *Sustainable Environ. Res.*, 2019, **29**, 5.
7 E.-H. Ablouh, R. Jalal, M. Rhazi and M. Taourirte, *Int. J. Biol. Macromol.*, 2020, **151**, 492–498.
8 Y. Yang, Y. Lu, K. Zeng, T. Heinze, T. Groth and K. Zhang, *Adv. Mater.*, 2020, 2000717.
9 A. M. Youssef, M. A. El-Samahy and M. H. Abdel Rehim, *Carbohydr. Polym.*, 2012, **89**, 1027–1032.
10 D. Klemm, B. Philipp, T. Heinze, U. Heinze and W. Wagenknecht, *Comprehensive Cellulose Chemistry*, Wiley, 1998, vol. 2.
11 N. Reddy and Y. Yang, *Green Chem.*, 2005, **7**, 190.
12 A. Essaghraoui, K. Khatib, B. Hamdaoui, F. Brouillette, E.-H. Ablouh and A. Belfkira, *J. Pharm. Innovation*, 2021, 1–11.
13 N. Gospodinova, A. Grelard, M. Jeannin, G. C. Chitanu, A. Carpov, V. Thiéry and T. Besson, *Green Chem.*, 2002, **4**, 220–222.

14 A. Zyane, E. Ablouh, E. M. Sabbar, F. Brouillette and A. Belfkira, *Heliyon*, 2020, **6**, e04977.
15 X. Zeng, L. Deng, Y. Yao, R. Sun, J. Xu and C.-P. Wong, *J. Mater. Chem. C*, 2016, **4**, 6037–6044.
16 S. Chaouf, S. El Barkany, H. Amhamdi, I. Jilal, Y. El Ouardi, M. Abou-salama, M. Loutou, E.-H. Ablouh, H. El Ouarghi and A. El Idrissi, *Mater. Today: Proc.*, 2020, **31**, S175–S182.
17 S. Chaouf, S. El Barkany, I. Jilal, Y. El Ouardi, M. Abou-salama, M. Loutou, A. El-Houssaine, H. El-Ouarghi, A. El Idrissi and H. Amhamdi, *J. Water Process. Eng.*, 2019, **31**, 100807.
18 I. Jilal, S. El-Barkany, Z. Bahari, O. Sundman, A. El-Idrissi, M. Abou-Salama, M. Loutou, E. Ablouh and H. Amhamdi, *Mater. Today: Proc.*, 2019, **13**, 909–919.
19 P. L. Granja, L. Pouységu, M. Pétraud, B. De Jéso, C. Baquey and M. A. Barbosa, *J. Appl. Polym. Sci.*, 2001, **82**, 3341–3353.
20 N. Inagaki, S. Nakamura, H. Asai and K. Katsuura, *J. Appl. Polym. Sci.*, 1976, **20**, 2829–2836.
21 D. M. Suflet, G. C. Chitanu and V. I. Popa, *React. Funct. Polym.*, 2006, **66**, 1240–1249.
22 Y. Shi, D. Belosinschi, F. Brouillette, A. Belfkira and B. Chabot, *Carbohydr. Polym.*, 2014, **106**, 121–127.
23 Y. Noguchi, I. Homma and T. Watanabe, *Cellulose*, 2020, **27**, 2029–2040.
24 F. Rol, C. Sillard, M. Bardet, J. R. Yarava, L. Emsley, C. Gablin, D. Léonard, N. Belgacem and J. Bras, *Carbohydr. Polym.*, 2020, **229**, 115294.
25 S. Zhang, H. Chen, Y. Zhang, Y. Zhang, W. Kan and M. Pan, *Polymers*, 2020, **12**, 336.
26 N. Li, J. Ming, R. Yuan, S. Fan, L. Liu, F. Li, X. Wang, J. Yu and D. Wu, *ACS Sustainable Chem. Eng.*, 2020, **8**, 290–301.
27 K. Al Hokayem, R. El Hage, L. Svecova, B. Otazaghine, N. Le Moigne and R. Sonnier, *Molecules*, 2020, **25**, 1629.
28 F. Rol, N. Belgacem, V. Meyer, M. Petit-Conil and J. Bras, *Cellulose*, 2019, **26**, 5635–5651.
29 X. Luo, J. Yuan, Y. Liu, C. Liu, X. Zhu, X. Dai, Z. Ma and F. Wang, *ACS Sustainable Chem. Eng.*, 2017, **5**, 5108–5117.
30 P. Liu, P. F. Borrell, M. Božič, V. Kokol, K. Oksman and A. P. Mathew, *J. Hazard. Mater.*, 2015, **294**, 177–185.
31 F. Carosio, M. Ghanadpour, J. Alongi and L. Wågberg, *Carbohydr. Polym.*, 2018, **202**, 479–487.
32 F. Rol, M. N. Belgacem, A. Gandini and J. Bras, *Prog. Polym. Sci.*, 2019, **88**, 241–264.
33 Y. Shi, D. Belosinschi, F. Brouillette, A. Belfkira and B. Chabot, *BioResources*, 2015, 4375–4390.
34 J. D. Reid and L. W. Mazzeno, *Ind. Eng. Chem.*, 1949, **41**, 2828–2831.
35 N. Illy, M. Fache, R. Ménard, C. Negrell, S. Caillol and G. David, *Polym. Chem.*, 2015, **6**, 6257–6291.
36 G. Nourry, D. Belosinschi, M. P. Boutin, F. Brouillette and R. Zerrouki, *Cellulose*, 2016, **23**, 3511–3520.
37 R. K. Jain, K. Lal and H. L. Bhatnagar, *J. Appl. Polym. Sci.*, 1985, **30**, 897–914.
38 P. L. Granja, L. Pouységu, D. Deffieux, G. Daudé, B. De Jéso, C. Labrugère, C. Baquey and M. A. Barbosa, *J. Appl. Polym. Sci.*, 2001, **82**, 3354–3365.
39 M. Nguyen, M. Al-Abdul-Wahid, K. Fontenot, E. Graves, S. Chang, B. Condon, C. Grimm and G. Lorigan, *Molecules*, 2015, **20**, 11236–11256.
40 F. Niu, N. Wu, J. Yu and X. Ma, *Carbohydr. Polym.*, 2020, **242**, 116422.
41 H. El Omari, E. Ablouh, F. Brouillette, M. Taourirte and A. Belfkira, *Cellulose*, 2019, **26**, 9295–9309.
42 T. Petreus, B. A. Stoica, O. Petreus, A. Goriuc, C.-E. Cotrutz, I.-V. Antoniac and L. Barbu-Tudoran, *J. Mater. Sci.: Mater. Med.*, 2014, **25**, 1115–1127.
43 M. Božič, P. Liu, A. P. Mathew and V. Kokol, *Cellulose*, 2014, **21**, 2713–2726.
44 W. D. Wanrosli, R. Rohaizu and A. Ghazali, *Carbohydr. Polym.*, 2011, **84**, 262–267.
45 D. Aoki and Y. Nishio, *Cellulose*, 2010, **17**, 963–976.
46 M. R. Mucalo, K. Kato and Y. Yokogawa, *Colloids Surf., B*, 2009, **71**, 52–58.
47 N. K. Yurkshtovich, T. L. Yurkshtovich, F. N. Kaputskii, N. V. Golub and R. I. Kosterova, *Fibre Chem.*, 2007, **39**, 31–36.
48 V. Kokol, M. Božič, R. Vogrinčič and A. P. Mathew, *Carbohydr. Polym.*, 2015, **125**, 301–313.
49 M. Ghanadpour, B. Wicklein, F. Carosio and L. Wågberg, *Nanoscale*, 2018, **10**, 4085–4095.
50 B. J. Cade-Menun, *Talanta*, 2005, **66**, 359–371.
51 J. Lehtonen, J. Hassinen, A. A. Kumar, L.-S. Johansson, R. Mäenpää, N. Pahimanolis, T. Pradeep, O. Ikkala and O. J. Rojas, *Cellulose*, 2020, **27**, 10719–10732.
52 M. C. Popescu, C. Ungureanu, E. Buse, F. Nastase, V. Tucureanu, M. Suchea, S. Draga and M. A. Popescu, *Appl. Surf. Sci.*, 2019, **481**, 1287–1298.
53 O. Petreu, T. Bubulac, I. Petreu and G. Cazacu, *J. Appl. Polym. Sci.*, 2003, **90**, 327–333.
54 A. Naderi, T. Lindström, G. Flodberg, J. Sundström, K. Junel, A. Runebjörk, C. F. Weise and J. Erlandsson, *Nord. Pulp Pap. Res. J.*, 2016, **31**, 20–29.
55 Y. Noguchi, I. Homma and Y. Matsubara, *Cellulose*, 2017, **24**, 1295–1305.
56 A. A. Kadam, S. Lone, S. Shinde, J. Yang, R. G. Saratale, G. D. Saratale, J.-S. Sung, D. Y. Kim and G. Ghodake, *ACS Sustainable Chem. Eng.*, 2019, **7**, 5764–5775.
57 F. Xu, L. Zhong, C. Zhang, P. Wang, F. Zhang and G. Zhang, *ACS Sustainable Chem. Eng.*, 2019, **7**, 13999–14008.
58 I. van der Veen and J. de Boer, *Chemosphere*, 2012, **88**, 1119–1153.
59 B. Boinon, A. Belfkira, M. Camps and J.-P. Monthéard, *Makromol. Chem. Rapid Commun.*, 1984, **5**, 477–482.
60 D. K. Shen and S. Gu, *Bioresour. Technol.*, 2009, **100**, 6496–6504.
61 X. Zhang, W. Yang and C. Dong, *J. Anal. Appl. Pyrolysis*, 2013, **104**, 19–27.
62 C. E. Higgins and W. H. Baldwin, *Anal. Chem.*, 1955, **27**, 1780–1783.